N93-26192

# The X-ray Reflectivity of the AXAF VETA-I Optics

E. Kellogg, G. Chartas, D. Graessle, J. P. Hughes, L. Van Speybroeck, P. Zhao
Harvard/Smithsonian Center for Astrophysics
60 Garden Street
Cambridge, MA 02138

M. C. Weisskopf, R. F. Elsner, S. L. O'Dell
Space Science Laboratory
George C. Marshall Space Flight Center
Huntsville, AL 35812

## ABSTRACT

The x-ray reflectivity of the VETA-I optic, the outermost shell of the AXAF x-ray telescope, with a bare Zerodur surface, is measured and compared with theoretical predictions. Measurements made at energies of 0.28, 0.9, 1.5, 2.1, and 2.3 keV are compared with predictions based on ray trace calculations. The data were obtained at the x-ray calibration facility at Marshall Space Flight Center with an electron impact x-ray source located 528 m from the grazing incidence mirror. The source used photoelectric absorption filters to eliminate bremsstrahlung continuum. The mirror has a diameter of 1.2 m and a focal length of 10 m. The incident and reflected x-ray flux are detected using two proportional counters, one located in the incident beam of x-rays at the entrance aperture of the VETA-I, and the other in the focal plane behind an aperture of variable size. Results on the variation of the reflectivity with energy as well as the absolute value of the reflectivity are presented. We also present a synchrotron reflectivity measurement with high energy resolution over the range 0.26 to 1.8 keV on a flat Zerodur sample, done at NSLS. We present evidence for contamination of the flat by a thin layer of carbon on the surface, and the possibility of alteration of the surface composition of the VETA-I mirror perhaps by the polishing technique. The overall agreement between the measured and calculated effective area of VETA-I is between 2.6% and 10%, depending on which model for the surface composition is adopted. Measurements at individual energies deviate from the best-fitting calculation to 0.3 to 0.8%, averaging 0.6% at energies below the high energy cutoff of the mirror reflectivity, and are as high as 20.7% at the cutoff. We also discuss the approach to the final preflight calibration of the full AXAF flight mirror.

## 1. INTRODUCTION

In the following sections we discuss the techniques we used for the measurement of VETA-I effective area. We also discuss the techniques used for calculation of the predicted effective area from previously existing knowledge of the composition of the reflecting surface material, atomic scattering coefficients, and the geometry of the mirrors. We present a summary of the raytrace calculation procedure, and give the results of the comparison, compared with the data. We also present the results of the synchrotron reflectivity measurement for comparison.

The total effective area is defined in this work as the integral of the point response function (PRF) over the back hemisphere of solid angle behind the optics. For observations with the AXAF observatory, one could consider whether this is really a useful quantity. It is of interest when comparing total reflected power with that predicted from scattering theory, but the scattering theory uses scattering coefficients obtained from experiments that are difficult to do precisely. Experimental measurements of reflection are very difficult to do out to scattering angles of $\pi/2$ because the flux density is so low at large angles, and the geometry of the optics prevents rays scattered at angles larger than about one degree from reaching the focal plane. Other measurements, such as total absorption, are also difficult. In this paper, we report estimates of the total effective area to $\pi/2$ based on extrapolation of measurements taken out to angles up to 17.5 arcmin, at which point the flux density is less than $10^{-10}$ of its peak central value.

## 2. MEASUREMENT TECHNIQUE

The general aspects of the VETA-I test are described by Kellogg et al[1]. The measurement technique uses photometric x-ray detectors[2] with a series of circular mechanical apertures of increasing diameter centered on the peak of the PRF to define the geometric flux collecting area. The size of each aperture corresponds to an angle from the center of the point response function, out to which all flux is integrated. The largest aperture used was 20 mm diameter, which corresponds to 3.3 arcmin radius. At larger angles, the aperture was moved off-center from the PRF peak to measure the flux outside the maximum centered angle. These were known as wing scans.

The x-ray source is described in Chartas et al[2] and Zhao et al[3]. The targets used and resulting characteristic line energies are given in Table 1. The dominant line is $\alpha_1$ in Siegbahn notation which corresponds to either the transition $KL_{III}$ or $L_{III}M_V$.

The technique of Chartas et al[2] is used to define the x-ray energy. The contribution to the reflected flux from the VETA-I optic due to continuum from the x-ray source is subtracted, using a model of the mirror reflectivity vs. energy. What remains after the subtraction is the contribution from the characteristic line(s).

The apertures used are nominally circular with diameters ranging from 0.005 to 20 mm. The actual sizes and shapes deviate from ideal circles, so this effect must be taken into account. The details of these size and shape measurements are

described by Podgorski et al[4].

Table 1: X-ray targets and Energies

| Element | Z | Shell | Dominant Line Energy, keV | Mean Line Energy, keV |
|---|---|---|---|---|
| C | 6 | K | 0.277 | 0.277 |
| Cu | 29 | L | 0.9297 | 0.932 |
| Al | 13 | K | 1.4867 | 1.488 |
| Zr | 40 | L | 2.04236 | 2.067 |
| Mo | 42 | L | 2.29316 | 2.334 |

A number of runs were carried out with the same x-ray target at different electron currents in order to determine the sensitivity of the results to the intensity of the X-ray beam. The error from such an effect was found to be much smaller than other errors.

Absolute normalization of the effective area was determined by taking the ratio of the flux in the x-ray line in the XDA detector to the flux in the x-ray line in the BND detector and multiplying by the open area of the BND detector, a 20 mm diameter aperture whose area was measured to be $100\pi = 314.16 \pm 0.08$ mm$^2$ ($\pm$ 0.025%). [4]. That error is negligible in comparison with others, and so is ignored in the error analysis.

## 3. CALCULATION OF TOTAL REFLECTED ENERGY

We define the effective area as the integral of the PRF with the energy spectrum of the x-ray source, and the integral over angles with respect to the incident beam direction $0 < \theta < \pi/2$ and $0 < \phi < 2\pi$, polar and azimuthal angles, respectively. In this paper, we assume the PRF not to be a function of $\phi$. We also assume that the PRF is composed of two functions of $\theta$, a core $f_c(\theta)$ and a wing. We find that to a sufficient approximation[5], the wing has a power law distribution $f_w(\theta) = K\theta^{-\alpha}$. The functional form of the PRF at large angles is obtained from a fit to the wing scan data, such as from Figure 1. Therefore, the integral of the PRF, or the Effective Area out to $\pi/2$ is

$$EffectiveArea = Core(\theta_2) + Wing(\theta_1)$$

$$\cong \int_0^{\theta_2} f_c(\theta)\,\theta d\Omega + \int_{\theta_1}^{\pi/2} (K\theta^{-\alpha})\,d\Omega$$

where $\theta_1$ is the angle at which the contribution of the wing to the PRF is very small compared with the core and $\theta_2$ is the angle at which the contribution of the core is very small compared to the wing. The wing is then

$$Wing(\theta_1) = \int_0^{2\pi} \int_{\theta_1}^{\pi/2} K\theta^{-\alpha} \sin\theta d\theta d\phi$$

$$= 2\pi K \int_{\theta_1}^{\pi/2} \theta^{-\alpha} \sin\theta d\theta \cdot$$

In Figure 1, we show the PRF of the VETA-I mirror at Al-K, 1.49 keV. The data at angles from $4.7 \times 10^{-6}$ to $9 \times 10^{-4}$ rad were taken using annular apertures consisting of an open annulus of a circle cut in solid metal, with four spokes to support the central opaque circle. The annulus has an inner diameter 0.9 of its outer diameter. The spokes obscure 10% of the

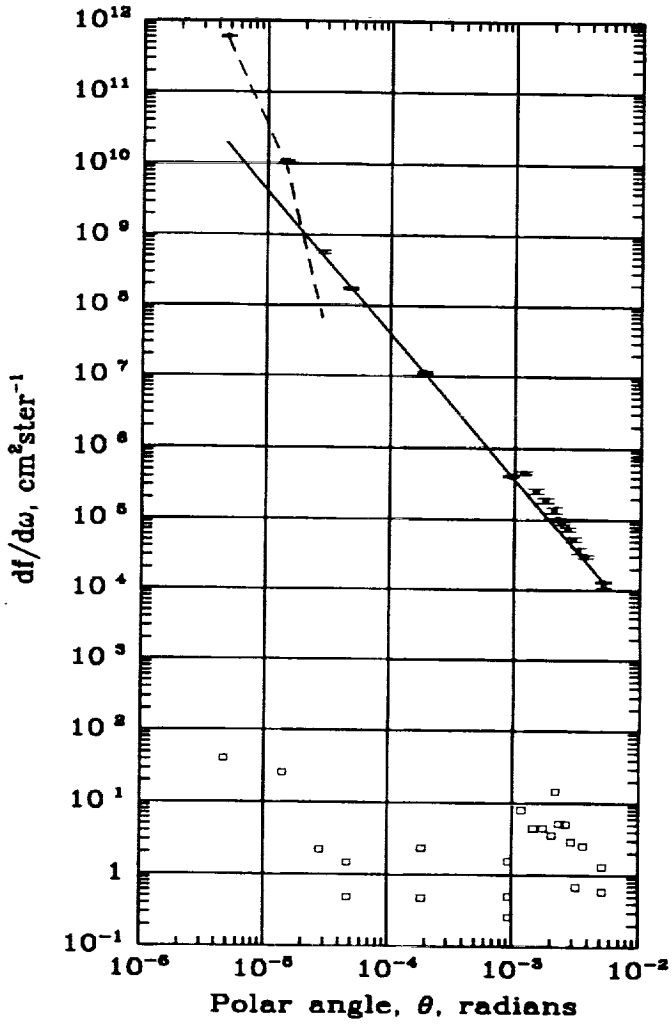


Figure 1. PRF of VETA-I at 1.49 keV. The open circles are the measured PRF, with 1 $\sigma$ error bars. The open squares are the deviations of the PRF from the power law fit to the wings of the PRF, which is the line of constant slope. The dashed line is the core PRF with the wing fit subtracted.

annulus at angles of 45° with the horizontal and vertical axes. At larger angles out to $5.2 \times 10^{-3}$ rad, circular pinhole apertures offset from the center of the PRF were used. In Figure 1 a power law fit to the data at large angles is shown. The slope of the function with θ is given in Table 2. The equation fitted is $\log PRF = -\alpha \log\theta + \log b$ . That component was subtracted from the PRF measured at the three smaller angles, resulting in the steeply rising curve in Figure 1 at small angles. The fit to the data was done only to the annuli data, since the pinholes must be corrected by a factor that depends on the ratio of their distance off axis to their size, and on the power law slope. The pinhole points lie above the curve, but approach it at larger angles, as the correction becomes smaller.

Therefore, we see that

- the PRF contains an outer component that is reasonably well represented by a power law
- the transition to the steeper inner component occurs at angles less than $10^{-4}$ rad.

As a result, it appears reasonable to use the power law to estimate the flux contained in the portion of the PRF outside the 20 mm pinhole (which subtends a half-angle of $9.8 \times 10^{-4}$ rad).

The results of the wingscans at the other four energies are shown in Figure 2. The parameters of the logarithmic fits to the outer part of the PRF are also listed in Table 2. The slopes in Table 2 for the three middle energies, 0.93, 1.49 and 2.06 keV, are not significantly different, but the slope at 0.277 keV is significantly steeper, and the slope at 2.29 keV appears to be flatter, although it is based on only four data points. The slope is a result of the size distribution of features in the microroughness of the surface, as well as of any possible dust contamination that lies on the surface. This result suggests that some information about the size distributions may ultimately be obtained from the wing scans.

Table 2: Power Law Fits to the Outer Wings of the PRF

| Line | Energy keV | α | log b | Reduced $\chi^2$ |
|---|---|---|---|---|
| C K | 0.277 | 2.381 ± 0.007 | -1.904 ± 0.025 | 13.9 |
| Cu L | 0.930 | 2.004 ± 0.011 | -0.488 ± 0.034 | 3.2 |
| Al K | 1.49 | 2.028 ± 0.007 | -0.522 ± 0.023 | 4.3 |
| Zr L | 2.06 | 2.074 ± 0.046 | -1.24 ± 0.16 | 1.4 |
| Mo L | 2.29 | 1.643 ± 0.075 | -0.578 ± 0.215 | 4.6 |

The large values of reduced $\chi^2$ for the power law fits may come from a lack of azimuthal symmetry in the wings of the PRF, or because the model chosen doesn't fit the data well enough. For the Cu-L data, we did fits to the wing scans at four azimuths corresponding to scans in the vertical and horizontal directions, and the slopes were the same within error, but the normalizations differed by almost a factor of two. We attempted to improve the Al fit by averaging over azimuth before fitting, but no significant improvement resulted.

We note that the fractional power in the wings increases with energy, as expected from scattering.

## 4. CHARACTERISTICS OF ZERODUR: COMPOSITION

In order to compare the measured effective area with that expected, we calculate the effective area from tabulated atomic scattering factors. Such a calculation can only be done if the composition of the reflecting surface is known. We initially assumed that the surface has the same composition as the bulk material. The Zerodur used to construct the AXAF mirrors was supplied by Schott. The composition is given in Table 3, in descending order of abundance[6].

Table 3: Composition of AXAF Zerodur Mirrors

| Compound | Fraction by weight | Compound | Fraction by weight |
|---|---|---|---|
| $SiO_2$ | 0.555 | $ZrO_2$ | 0.019 |
| $Al_2O_3$ | 0.253 | ZnO | 0.014 |
| $P_2O_5$ | 0.079 | MgO | 0.010 |
| $Li_2O$ | 0.037 | $Na_2O$ | 0.005 |
| $TiO_2$ | 0.023 | $As_2O_3$ | 0.005 |

## 5. RAY TRACE CALCULATIONS

The effective area of the VETA-I was calculated using the OSAC raytrace code[7]. It was assumed that the optical elements were perfectly aligned, the despace was 109.03 mm and the X-ray source was on-axis. The actual finite source distance of 518160 mm (1730 ft.) was used. The reflectivity of Zerodur was calculated using the Henke et al[8] optical constants for the mixture shown in Table 3 with a bulk density value of 2.53 g $cm^{-3}$.

There are stops along the optic axis defining the axial extent of the reflecting surfaces. The stops are: the apodizer located at the back of the P1, the mid-plane aperture plate, and the apodizer located at the back of the H1. However, due to the finite source distance and despace of the P1 and H1, only about 60% of the nominal flight length of the P1 optic was exposed, so the mechanical stops were not significant.

The figure of each optic was assumed to be a perfect conic section with the as-designed conic parameters. The large scale figure errors, either due to fabrication or to gravitational or thermal distortions, do not have any significant effect on calculations of total reflectivity in $2\pi$ ster, since they only redistribute power in the core of the PRF. Small scale microroughness and dust on the surface can have a significant effect, however.

Because of the assumptions of perfect alignment, an on-axis source position, and no distortion, and because we did not

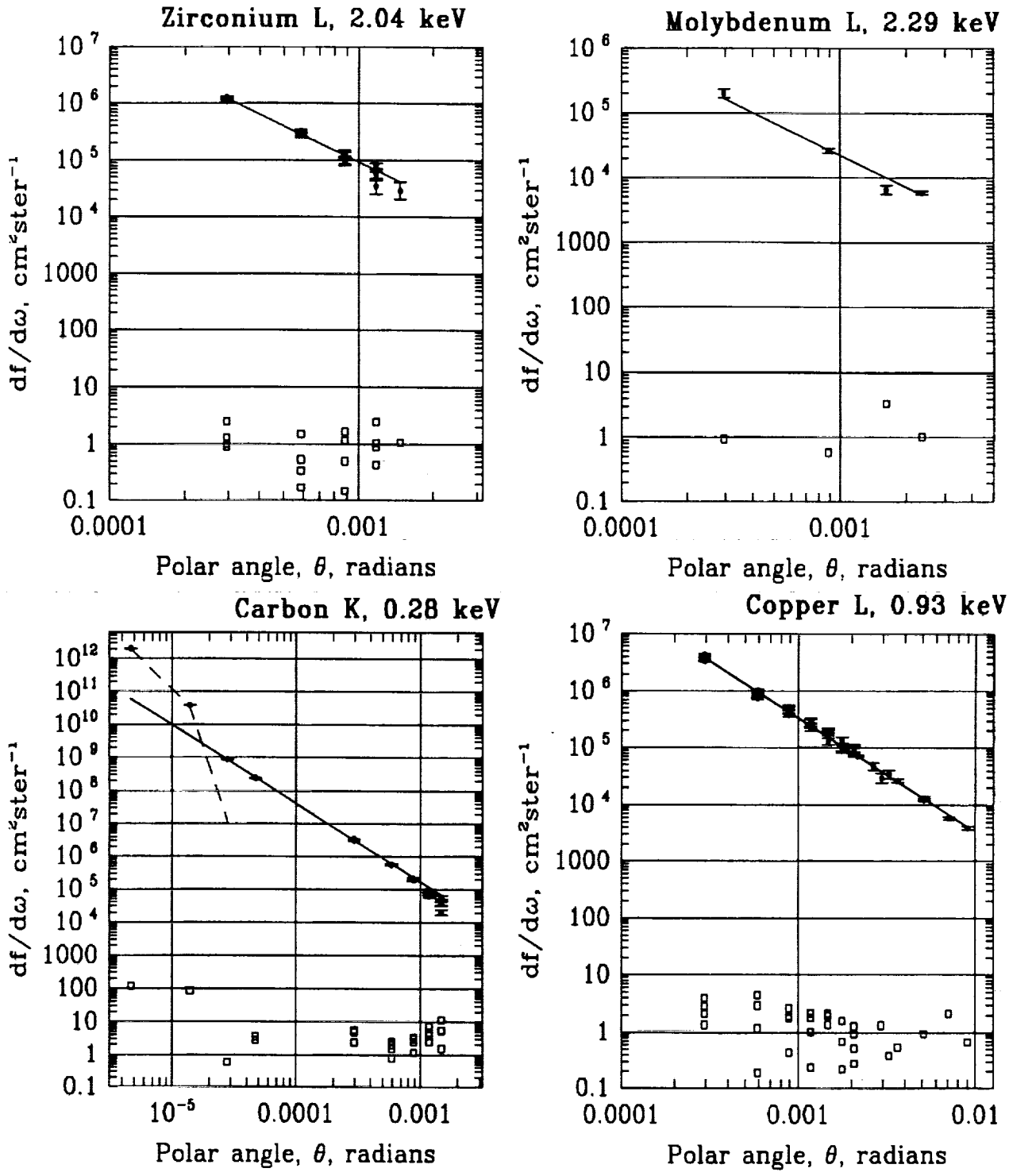


Figure 2. PRF of VETA-I at the four remaining energies. The circles are the measured PRF, with 1 σ error bars. The open squares are the deviations of the PRF from the power law fit to the wings of the PRF, which is the line of constant slope. The dashed line for carbon-K is the core PRF with the wing fit subtracted.

do a detailed model of the azimuthal dependence of the obscuration by the support struts, the raytrace had rotational symmetry about the optical axis. Consequently it was possible to reduce the integration over the entrance pupil of the telescope to a one dimensional radial integration. This was implemented by placing 2000 rays at a single angular position over an annular entrance pupil. The emerging rays were collected in a ray file, which was then filtered at the focal plane to determine which ones passed through a specified pinhole aperture, to determine the fraction that were transmitted.

We quote the total effective area over $2\pi$ ster, that is, integrated over the entire focal plane. Obscuration due to the four mirror support struts (which were 76.2 mm thick) reduced the calculated area by 8%. The results showed some dependence of the flux in the wings on azimuth which may be due to the struts.

## 6. ATOMIC SCATTERING FACTORS

The x-ray reflection coefficients were calculated using the most recent Henke et al atomic scattering factors[8], which are obtained by fitting a large quantity of experimental data. The factors are given as values of $f_1$ and $f_2$ from 10 to 30000 eV in logarithmic intervals, and represent the best available basis for comparison with previous measurements. Expressions for reflection from scattering coefficients are given in the original Henke et al[9] paper.

## 7. RESULTS

Figure 3 shows the effective area of the VETA-I, calculated using the methods described above, for several variations on the composition of the glass. These results were then compared with the measured effective area to see which composition would give the best fit to the measurements. The structure in the calculated curve due to edges of oxygen (532 eV), aluminum (1560 eV) and silicon (1840 eV), which are the main constituents of Zerodur, is readily apparent.

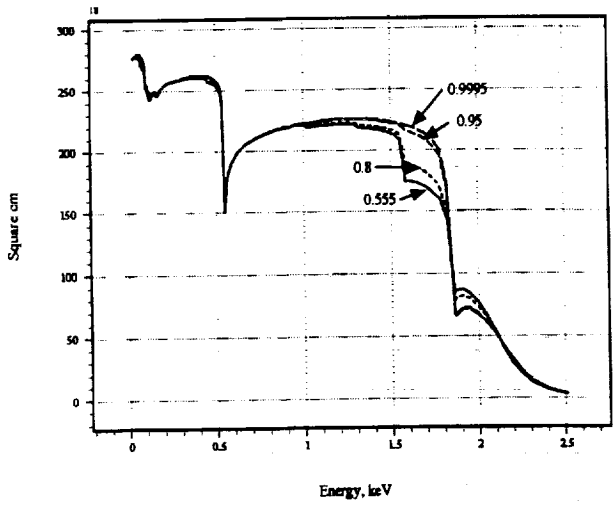


Figure 3. Calculated effective area of VETA-I for four different compositions. The labels indicate the fractional composition of $SiO_2$. The nominal composition for Zerodur is 0.555.

The comparison between calculated and measured effective area is shown in Figure 4. The calculated curves were normalized to the measured points by minimizing $\chi^2$. The calculated area was multiplied by 0.974 for the pure $SiO_2$, and 1.10 for Zerodur to obtain the minimum $\chi^2$. Thus, there is a slight preference for the surface composition of the glass being pure $SiO_2$, rather than Zerodur, based on the better $\chi^2$ (20 for 4 d.o.f. vs. 51 for Zerodur) and normalization.

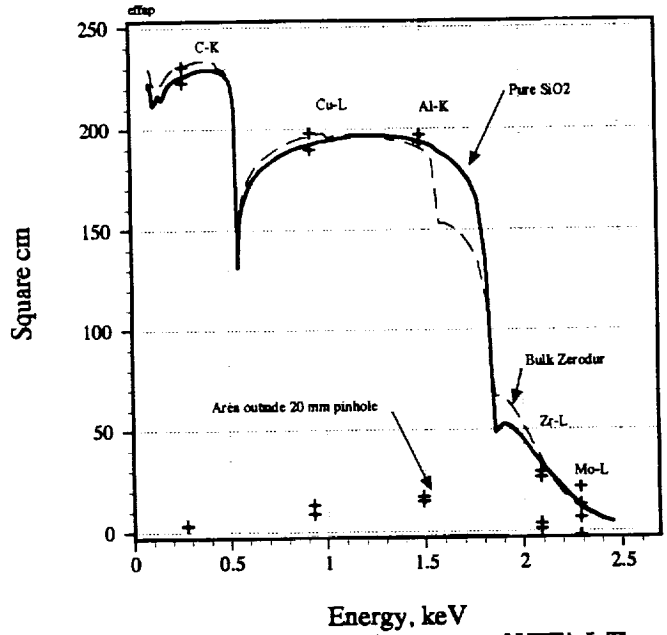


Figure 4. Calculated and measured effective area of VETA-I. The crosses are the measured results, giving the upper and lower limits of the estimated 1σ errors. In addition to the total effective area, the area outside the 20 mm pinhole, or 1 mrad angle, is plotted, which shows that the wings of the PRF are more important at higher energy.

A similar plot of the calculated effective area compared with the measured data is shown in Figure 5, for the case of Zerodur with a range of thicknesses of carbon from 0 to 80 A. The measured effective area at 0.277 keV agrees best with the curve for no carbon layer.

## 8. SYNCHROTRON REFLECTIVITY MEASUREMENTS

The x-ray reflectivity of a flat polished sample (P1-1) of the VETA-I P1 paraboloid section material was measured at the NSLS, using techniques described by Graessle et al[10]. Figure 6 shows the results, compared with a calculation based on the Henke tables[8]. Obvious absorption features are present from carbon (284 eV), oxygen (532 eV), and aluminum (1560 eV). Incidentally, it is not surprising that the oxygen feature is much deeper than the Henke prediction; the latter are based on sparse data near edges. It should be noted that Figure 6 gives the reflectivity for *single* reflections from a *flat* mirror,

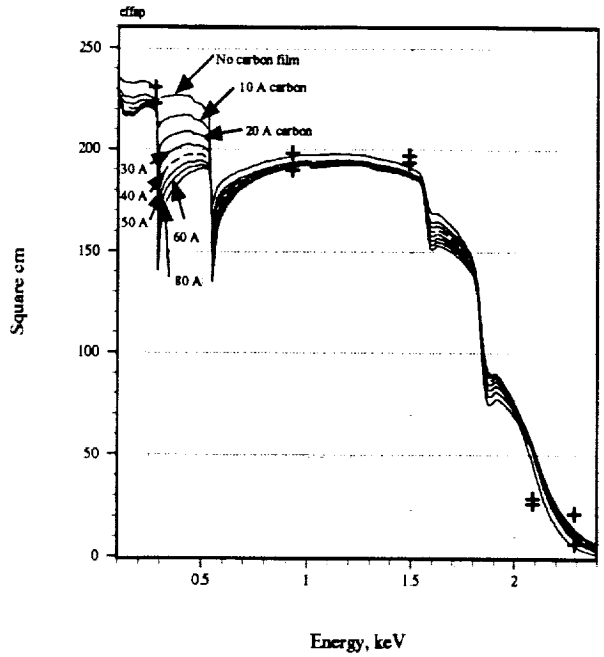


Figure 5. Calculated and measured effective area of VETA-I compared with calculations for Zerodur plus a thin film of hydrocarbon. A mean grazing angle approximation was used in this calculation.

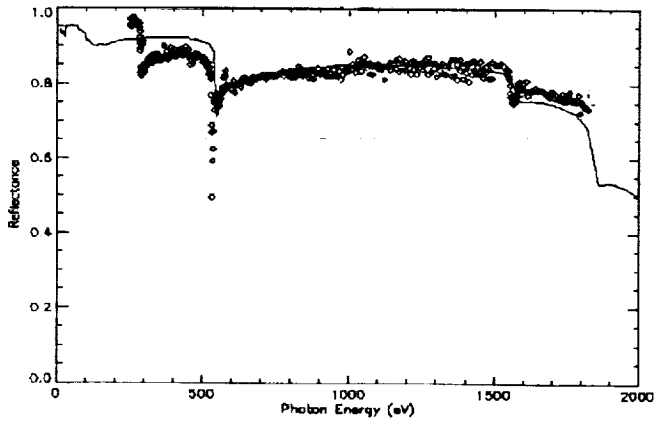


Figure 6. Reflectivity of P1-1 Zerodur sample flat, at an incident angle of 51.2 arcmin.

whereas the results in Figure 3, Figure 4 and Figure 5 are for *double* reflections from *the VETA-I optic*; while the same features are expected in both cases, their depth and gross energy dependences will differ.

There is a striking indication of the presence of carbon on the surface of the flat P1-1 sample, seen as the increase of reflectivity at energy below 284 eV, and the decrease above that energy, compared to the prediction for bare Zerodur.

## 9. DISCUSSION

### 9.1. Carbon contamination

The raytrace calculations for both Zerodur and pure $SiO_2$ are in good agreement with the measured effective area at 277 eV. We cannot yet make a statement with much certainty about the existence of hydrocarbon on the VETA-I, since the calculations we have done so far (see Figure 5) were only done with a mean grazing angle approximation, not a full raytrace. Also, It would be much better to have reflectivity measurements at energies just above and below the carbon edge to make the result less ambiguous.

For the flat, there is prima facie evidence for a carbon film. Therefore we conclude that the flat measured at the synchrotron was contaminated by carbon, and the VETA-I optic was probably not.

It is not surprising that the surface of the synchrotron test flat was contaminated by carbon, since no special prevention measures were taken. The VETA-I optic was, however, prepared under somewhat more stringent conditions, so it is again not surprising that the VETA-I shows no obvious contamination from a carbon film.

Carbon contamination will be important for AXAF operation in orbit, because such a film could be deposited at any time. If it happens before the final metal coating, it may interfere with proper adhesion at the least. If it happens after metal coating, the energy dependence of the PRF will be affected at the 5 - 10% level, much greater than our goal of 1-2% for knowledge of the PRF.

### 9.2. Possibility of changes in surface composition due to polishing

The formal $\chi^2$ analysis supports the notion of a pure $SiO_2$ surface, although we recognize that there are difficulties with interpreting the data, especially in estimating the total power outside the 20 mm diameter apertures. There is room for a more sophisticated analysis in the future that may give a less ambiguous interpretation.

The better agreement between the prediction for pure $SiO_2$ and the VETA-I measured reflectivity vs. energy could be due to a change of surface composition during polishing at HDOS, causing the enhancement of $SiO_2$. On the other hand, the synchrotron data from the flat show clear evidence for the Al edge at 1560 eV, so the polishing done at Marshall Space Flight Center did not affect the composition. The present VETA-I data and analysis ar not sufficient to allow firm conclusions to be drawn.

Changes in surface composition of the Zerodur may not be significant for the AXAF flight mirrors. They will be coated with a high density metal film to improve their x-ray reflectivity, which will not be significantly affected by the composition of the underlying Zerodur.

### 9.3. Absolute normalization

We have very little information on the error in our knowledge of the absolute geometric area. Two possible contributors are centering errors and errors in placement of apodizers.

The normalization factor needed to minimize $\chi^2$ for the fit in Figure 4 is 0.974 for pure $SiO_2$, and 1.10 for Zerodur, which

gives us an overall agreement in the product of geometric area and reflectivity of 2.6% and 10% respectively. We would like to believe the better agreeing number, and that this shows the geometric errors to be negligible, but of course, even if the better number is true, there could always be a fortuitous cancelling of geometric errors and overall reflectivity calculation errors. For the final flight calibration of AXAF, it will be important to devise a way to estimate these geometric errors, and include them in our analysis.

### 9.4. Implications for final AXAF preflight calibration

The value of $\chi^2$ for the best fit to the measured effective area, 20 for 4 d.o.f., is still not formally acceptable, so there is evidence for some remaining problem, which could be due to unknown errors in the measurement process, or in the calculations.

There is a great deal of structure expected in the reflectivity curve between 1800 and 2200 eV. If we had measured reflectivity of flats polished in the identical manner to the VETA-I using the synchrotron over that energy range, we probably could have resolved the composition issue. We may be able to do this on a Zerodur sample when the VETA-I is disassembled and cut to the proper length for the flight AXAF optics.

In Table 4, we show the deviations between the measured values of the VETA-I effective area from Figure 4 and the best fit calculation at each of the energies. The average value of the deviations from the full area is 1.2%, which is one measure of how accurately we have done the measurement. Another measure is the normalization factor, which gives us an overall agreement in the product of geometric area and reflectivity of 2.6% for our best fit composition of pure $SiO_2$. Therefore, we might surmise that in orbital operation (assuming we make no improvement in our measuring techniques prior to the final flight calibration planned for 1995-96), AXAF could make measurements of absolute flux over a broad spectral band to ~1%, but in a pessimistic view, might be in error as much as 10% of the geometric area overall. At higher energies, where the reflectivity cuts off and the effective area is much smaller, the errors could be larger, as high as ~ 20%, as shown in the fourth column of Table 4.

Careful analysis of the calibration data and comparison with complete synchrotron reflectivity energy scans taken on faithful witness flats may reduce the errors at selected energies by allowing us to weight the individual measurements appropriately. For the final calibration, we are also planning to use

Table 4: Effective Area Deviation vs. Energy

| Energy keV | Line | Deviation from Measured Value to Best Fit, | |
|---|---|---|---|
| | | normalized to full area at 0.277 keV | normalized to area at each energy |
| 0.277 | C-K | 0.3% | 0.3% |
| 0.93 | Cu-L | 0.7% | 0.8% |
| 1.49 | Al-K | 0.6% | 0.7% |
| 2.09 | Zr-L | 2.5% | 20.7% |
| 2.29 | Mo-L | 0.6% | 8% |

detectors with considerably better energy resolution, eliminating errors due to contamination from continuum in the spectrum of the x-ray beam used at the calibration facility. The single worst disagreeing measured data point was at 2.09 keV, Zr-L. We know that this measurement suffered from by far the highest contamination by bremsstrahlung continuum, about 33%, compared to values as low as about 8% at other energies.

We also plan to characterize the nature of the x-ray beam's spectrum much more carefully using high resolution spectrometers. We believe all three of these improvements are necessary to achieve the desired accuracy of effective area calibration, even up to the high energy cutoff of the mirror.

## 10. ACKNOWLEDGMENTS

There were many people at SAO, NASA, Hughes Danbury Optical Systems, TRW and Eastman Kodak who made this measurement possible. A few that we worked closely with and have not been recognized elsewhere are John Cobuzzi, Kathy Flanagan, John McDougal, John Roll, Dave Watson, and Marty Zombeck.

This work was partially supported under NASA Contract # NAS8-36123.

## 11. REFERENCES

1. E. Kellogg, R. Brissenden, K. Flanagan, M. Freeman, J. Hughes, M. Jones, M. Ljungberg, P. McKinnon, W. Podgorski, D. Schwartz, and M. Zombeck, "Calibration of the Verification Engineering Test Article-I (VETA-I) for AXAF using the VETA-I X-ray Detection System," *Proc. SPIE*, vol. 1546, pp.2-12, 1992.
2. G. Chartas, J. P. Hughes, E. M. Kellogg, M.V. Zombeck, M. K. Joy, J.J. Kolodziejczak, "Correcting x-ray spectra obtained from the AXAF VETA-I mirror calibration for pileup, continuum, background, and deadtime," *Proc. SPIE*, paper 1742-07, July 1992.

3. P. Zhao, E.M. Kellogg, D.A. Schwartz, M.A. Fulton, C>R. Bower, "Intensity distribution of the x-ray generator for the VETA-I test," *Proc. SPIE*, paper 1742-03, July 1992.
4. W.A. Podgorski, K.A. Flanagan, M.D. Freeman, E.M. Kellogg, T. Norton, P. Ouellette, A.G. Roy, D.A. Schwartz, "VETA-I x-ray detection system," *Proc. SPIE*, paper 1742-05, July 1992.
5. J. P. Hughes, D.A. Schwartz, A. Szentgyorgyi, L.P. Van Speybroeck, P. Zhao, "X-ray performance of the outer AXAF mirror pair based on measurements of the VETA-I ," *Proc. SPIE*, paper 1742-11, July 1992.
6. German patent Jurgen Petzoldt D1902432.
7. Optical Surface Analysis Code (OSAC). 1982.Perkin-Elmer Optical Technology Division, Danbury, CT.
8. B. L. Henke, E. M. Gullikson and J. C. Davis, Atomic Data and Nuclear Data Tables (to be published).
9. Henke, B.L., Lee, P., Tanaka, T.J., Shimabukuro, R.L., and Fujikawa, B.K. 1982, Atomic Data and Nuclear Data Tables 27, 1-144. Academic Press.
10. D.E. Graessle, J.C. Cobuzzi, E.M. Kellogg, D.A. Schwartz, R.L. Blake, P.P. Gong, "Reflectance calibrations of AXAF mirror samples at absorption edges using synchrotron radiation," *SPIE*, paper 1742-16, July 1992.